Environmental Science: Atmospheres

ROYAL SOCIETY OF CHEMISTRY

PAPER

View Article Online
View Journal | View Issue

Cite this: *Environ. Sci.: Atmos.*, 2022, **2**, 714

Ice nucleating properties of airborne dust from an actively retreating glacier in Yukon, Canada†

Yu Xi, [a] Cuishan Xu,[a] Arnold Downey, [b] Robin Stevens, [b] Jill O. Bachelder, ‡[b] James King, [c] Patrick L. Hayes *[b] and Allan K. Bertram *[a]

Received 7th December 2021
Accepted 14th May 2022

DOI: 10.1039/d1ea00101a

rsc.li/esatmospheres

Airborne dust from glacial outwash sediments may alter properties of clouds and climate at high latitudes by acting as ice nucleating particles (INPs). Nevertheless, the ice nucleating ability of airborne dust from glacial outwash sediments remains uncertain. To address this uncertainty, we measured the ice nucleating ability of airborne dust near an actively retreating glacier in Yukon, Canada during a period when airborne dust concentrations were well above background levels and most likely originated from glacial outwash sediments in the region. The airborne dust caused freezing at temperatures from −6 to −23 °C. Based on a heat assay and an ammonium sulfate assay, the INPs from the airborne dust that caused freezing at temperatures warmer than −15 °C likely contained biological materials. We show that airborne dust from the retreating glacier likely led to high concentrations of ice nucleating particles at the site for at least most of May 2018. These concentrations, at a freezing temperature of −15 °C, were approximately one order of magnitude higher than predictions using a global chemical transport model that included low latitude natural dust sources, but not natural high latitude dust sources.

Environmental significance

Airborne dust from glacial outwash sediments may alter properties of clouds and climate at high latitudes by acting as ice nucleating particles (INPs). Nevertheless, the ice nucleating ability of airborne dust from glacial outwash sediments remains uncertain. To address this uncertainty, we quantified the ice nucleating ability of airborne dust near an actively retreating glacier in Yukon, Canada. These results should be useful for predicting ice nucleating particles, and hence clouds and climate, at high latitudes.

1. Introduction

Ice nucleating particles (INPs) are particles that can initiate ice formation at temperatures between −35 and 0 °C.[1,2] Without INPs, clouds at temperatures between −35 and 0 °C would remain in a liquid state. Modelling studies have shown that the optical properties, lifetimes, and precipitation of clouds are sensitive to the concentrations and properties of INPs.[3–6] Hence, information on the concentrations, properties, and sources of INPs in the atmosphere is necessary to predict the Earth's radiative properties and hydrological cycle.

Recently, the concentrations, properties, and sources of INPs at high latitudes have received considerable attention,[7–15] in part, because temperatures in high latitude regions have increased at a faster rate than other regions and because clouds in these regions often form at temperatures less than 0 °C.[16,17] A potentially important source of INPs at high latitudes is glacial outwash sediments.[18,19] Glacial outwash sediments are formed when fine glacier flour is transported by meltwater and deposited at the terminus of glaciers. These sediments can then be emitted to the atmosphere by wind action forming airborne dust. As temperatures rise and ice and snow coverage decreases at high latitudes, airborne dust from glacial outwash sediments may increase in the future,[20,21] resulting in more INPs emitted into the atmosphere, and a potentially important climate feedback mechanism.[15] Nevertheless, studies on the ice nucleating properties of glacial outwash sediments or airborne dust from glacial outwash sediments are rare.

Tobo *et al.* showed that glacial outwash sediments collected on the ground in Svalbard have exceptional ice nucleating abilities, with the numbers of INPs per mass of material being around 5×10^3 g^{-1} at −5 °C and 7×10^8 g^{-1} at −20 °C. Such exceptional ice nucleating abilities are far superior to illite NX (a

[a]*Department of Chemistry, University of British Columbia, 2036 Main Mall, Vancouver, BC, V6T 1Z1, Canada. E-mail: bertram@chem.ubc.ca*

[b]*Department of Chemistry, University of Montreal, 1375 Avenue Thérèse-Lavoie-Roux, Montreal, QC, H2V 0B3, Canada. E-mail: patrick.hayes@umontreal.ca*

[c]*Department of Geography, University of Montreal, 1375 Avenue Thérèse-Lavoie-Roux, Montreal, QC, H2V 0B3, Canada*

† Electronic supplementary information (ESI) available. See https://doi.org/10.1039/d1ea00101a

‡ Present address: Department of Environmental Systems Science, ETH Zürich, Universitätstrasse 16, 8092 Zurich, Switzerland.

dust consisting of several minerals), likely due to a small amount of highly ice-active organic matter present in the sediments.[18] In contrast, Paramonov *et al.* showed that the ice nucleating abilities of glaciogenic silt collected from a glacial river in Iceland were similar to illite NX, kaolinite, and montmorillonite, all types of mineral dust, with the number of INPs per surface area of material being around 5×10^{-3} μm^{-2} at -30 °C and around 5×10^{-2} μm^{-2} at -35 °C.[22] Sanchez-Marroquin *et al.* showed that airborne Icelandic dust, which is often affected by the glacio-fluvial process, had ice nucleating abilities similar to K-feldspar, also a type of mineral dust, with the number of INPs per surface area around 5×10^{-6} μm^{-2} at -12.5 °C and 8×10^{-4} μm^{-2} at -25 °C.[19] While these studies have been crucial, studies at other locations are needed to determine if the exceptional ice nucleating abilities observed by Tobo *et al.* are common for airborne dust from glacial outwash sediments. Furthermore, only Sanchez-Marroquin *et al.* investigated the ice nucleating ability of airborne dust, while Tobo *et al.* and Paramonov *et al.* investigated the ice nucleating ability of surface-collected sediments or silts, which may have a different chemical composition, and hence ice nucleation ability, compared to airborne dust from sediments or silts. To illustrate, Bachelder *et al.* showed that PM10 elemental composition was enriched in trace elements as compared to bulk soil samples and the fine soil fractions (diameter < 53 μm) near the Kaskawulsh Glacier in Yukon, Canada. They proposed that this difference was because the primary mechanism for dust emission at the site was rupture of clay coatings on particles or the release of resident fine particulate matter trapped within sand particles.[23]

In the current study, we investigated the concentration of INPs and the ice nucleating ability of airborne dust at the A'äy Chù Delta (Fig. 1). This delta consists of glacial outwash sediments from the Kaskawulsh Glacier in Yukon, Canada, one of Canada's largest glaciers. Frequent dust storms occur in this region during spring and summer.[24] Furthermore, the retreat of the Kaskawulsh Glacier due to climate change recently caused an abrupt re-routing of meltwater from the Kaskawulsh Glacier in 2016 away from the A'äy Chù, leading to a decrease in A'äy Chù flow and an increase in the exposure of glacial outwash sediment during summer.[25]

Airborne dust samples were collected during May 2018, a period when the dust concentrations were very high (100 to 4000 μg m^{-3}) and the source of the dust was most likely glacial outwash sediments in the region (see below for details).[23] The ice nucleating ability of the airborne dust was determined in the immersion freezing mode, which is most relevant for mixed phase clouds in the atmosphere. The properties of the INPs were investigated using a heat assay and an ammonium sulfate assay. In addition to measuring concentrations of INPs at the site, we also compared concentrations of INPs at the site with concentrations predicted using a global chemical transport model that includes natural low latitude dust sources, but not natural high latitude dust sources.

2. Experimental

2.1. Sampling location, time, and method

Aerosol samples were collected near the Kaskawulsh Glacier in Yukon, Canada. The sampling location, referred to as the Down Valley site (60.9980, −138.5227),[23] is located on the A'äy Chù Delta (Fig. 1). The A'äy Chù originates from the Kaskawulsh Glacier, which has experienced active retreat due to climate change leading to a decrease in the size of the A'äy Chù in recent years.[25]

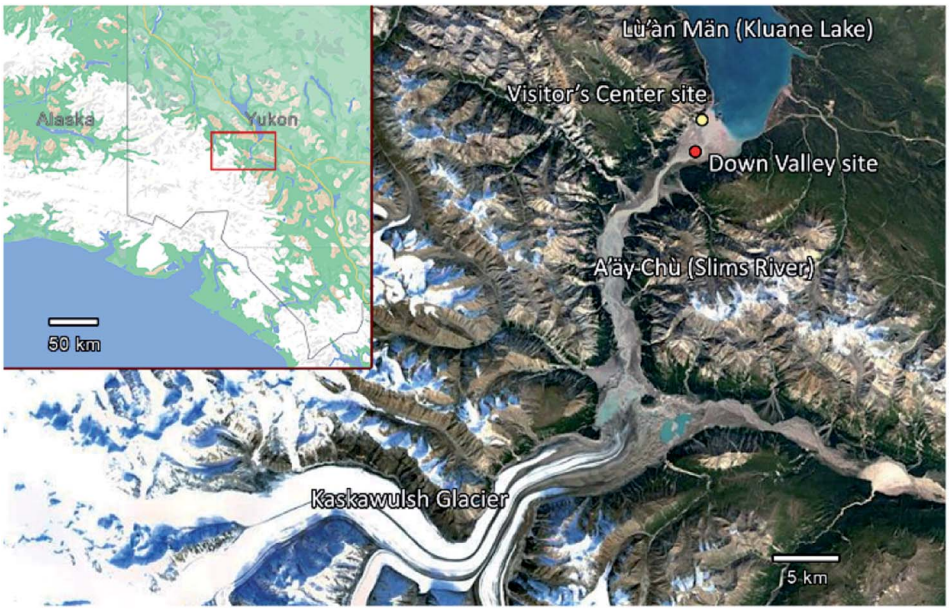

Fig. 1 Map of sampling location. Samples were collected from the Down Valley site, indicated by the red pin, located at the A'äy Chù Delta. Also shown is the nearby Visitor's Center, indicated by the yellow pin, where PM10 concentrations were also measured for comparison purposes. The insert map shows the location of the area in Yukon, Canada. The maps were taken from map data ©2021 Google.

Table 1 Relevant information on the ambient samples collected: sampling date, start time, sampling time, sampling mass (total mass of materials collected on the filter), and PM10 mass concentration (mass of aerosol particles with diameters less than 10 μm per volume of air)

Sampling date	Start time	Sampling time (h)	Sampled mass (mg)	PM10 mass concentration (μg m^{-3})
2018-May-15	09:09	20.77	16.74	1383.0
2018-May-16	06:07	28.50	14.05	844.8
2018-May-20	09:29	23.93	2.83	207.8
2018-May-22	09:19	24.93	8.53	596.9
2018-May-23	10:30	22.92	6.28	479.6
2018-May-24	09:37	23.80	6.92	506.1
2018-May-25	09:38	23.93	1.59	116.1

Aerosol samples from the Down Valley site were collected at a height of 6.1 m above ground level onto Nuclepore filters (Whatman® Nuclepore™ Track-Etched Membranes, 47 mm diameter, 0.4 mm pore size) using a mini-vol sampler (ARA instrument, Near-Federal Reference Method Sampler).[23] The mini-vol sampler was operated with a PM10 inlet and a flow rate of 10 L min^{-1}. The samples analyzed in the current study were collected on May 15, 16, 20, 22, 23, 24, and 25 in 2018. Specific dates and sampling times are given in Table 1. After collection, the filers were dried for 24 h in a desiccator and then the mass collected on each filter was determined gravimetrically. Since the samples were collected with a PM10 inlet, the measured mass concentrations correspond to PM10 concentrations (*i.e.* particulate mass concentrations with diameters less than 10 μm). After determining the PM10 concentrations, the filters were stored at −20 °C until used for the freezing measurements.

2.2. Extraction of the particles from the nuclepore filters

Prior to the freezing experiments and the size distribution measurements, the filters were added to plastic tubes (polypropylene) along with 5 mL of MilliQ water (distilled water further purified with a Millipore system, 18.2 MΩ cm at 25 °C). The plastic tubes were then shaken at 200 rpm for 1 hour by a platform shaker (New Brunswick Scientific, C2 platform shaker) to extract the particles from the filters. A similar method has been used previously to collect and extract ice nucleating particles.[26] After extraction, the ice nucleating ability of each suspension was tested immediately with the droplet freezing technique (see below). After testing the ice nucleation ability of each suspension, the size distributions of the particles within the suspensions were determined using a Coulter Counter (see below). The suspensions were stored at −20 °C after the freezing measurements and before the size distribution measurements.

2.3. Size distribution of particles in the extracted suspensions

The size distribution of particles in the extracted suspensions were measured using a Beckman Coulter™ Multisizer 4e Particle Analyzer (Coulter Counter), equipped with a 30 μm aperture tube. The Coulter Counter is a device designed for determining the concentration and size distributions of particles suspended in an electrolyte solution. As particles are drawn through microchannels that separate two chambers containing the electrolyte solution, each particle causes a brief change in the resistance of the liquid. The relationship between the measured change in electrical resistance and the size of the particles is used to determine the size of the particles.[27] For these experiments, aliquots of the suspensions were diluted by a factor of 50, 100, 150, or 200 in an electrolyte solution containing a dispersant (10 g L^{-1} of sodium hexametaphosphate dissolved in Isoton™). The dilution factor was adjusted in these experiments to avoid blockage of the instrument. This electrolyte solution was vacuum filtered twice through Nylaflo™ Nylon Membrane filters of 0.2 μm pore size before being used for dilutions. The blank-corrected size distributions of the diluted suspensions were then determined over the range of 0.6 to 18 μm. The aperture current was 400 μA, with a preamp gain of 4. The distributions were determined volumetrically, with the analyzer sampling 500 μL of diluted suspension each run, and three runs being averaged for each sample. The system was flushed between each run to prevent carry-over and samples containing the suspended particles were thoroughly agitated prior to transfers and analysis to prevent bias due to coagulation. The instrument was calibrated and verified for accurate particle sizing using NIST-traceable Coulter CC size standards of known diameters within the appropriate range for the 30 μm aperture, between 3 and 6 μm.

2.4. Droplet freezing experiments

The ice nucleating properties of the extracted suspensions were measured using the droplet freezing technique.[7,28–31] For each trial, three siliconized glass slides (18 mm, HR3-239, Hampton Research) were cleaned with MilliQ water, dried with nitrogen gas, and then placed on a cooling stage (Grant Asymptote EF600 freezer). The uncertainty in the temperature measurement of the cooling stage was ±0.25 °C, according to the manufacturer, which was confirmed using the melting temperatures measured for water and dodecane.[32] Approximately 60 droplets of suspension, with a volume of 1 μL each, were pipetted onto the glass slides. A chamber was placed over the cooling stage and a nitrogen gas flow (0.2 L min^{-1}) was passed through the chamber to prevent the condensation of water from the air while cooling the stage. The flow did not cause significant evaporation of the droplets based on the optical images, and the flow should not influence freezing temperatures according to a former study using a similar method.[33] The temperature of the

stage was decreased at a rate of 3 °C min^{-1} from 20 °C until all the droplets were frozen. The freezing process of the droplets was recorded and analyzed with a MATLAB script to obtain the frozen fraction of droplets at each temperature.[31] For this study, MilliQ water served as lab blanks and washing water from blank filters (processed using the same method as the sample filters) served as field blanks. To extend the temperature range of the freezing measurements, the extracted suspensions were also diluted by a factor of 10, and the freezing experiments were repeated on these diluted suspensions.

The number of INP per volume of suspension ($[\mathrm{INP}(T)]_{\mathrm{liquid}}$) was calculated using the equation below:

$$[\mathrm{INP}(T)]_{\mathrm{liquid}} = -\frac{N_0 \ln\left(\frac{N_{\mathrm{u}}(T)}{N_0}\right)}{V_{\mathrm{t}}} \quad (1)$$

where N_0 represents the total number of droplets, $N_{\mathrm{u}}(T)$ represents the number of unfrozen droplets at temperature T, and V_{t} represents the total volume of droplets in each trial.[34]

The $[\mathrm{INP}(T)]_{\mathrm{liquid}}$ values of the field blanks were subtracted from that of the suspensions to obtain the corrected $[\mathrm{INP}(T)]_{\mathrm{liquid}}$ values for the glacial samples. The corrected $[\mathrm{INP}(T)]_{\mathrm{liquid}}$ values were used to calculate the number of INP per volume of air, $[\mathrm{INP}(T)]_{\mathrm{air}}$, using the equation below:

$$[\mathrm{INP}(T)]_{\mathrm{air}} = \frac{[\mathrm{INP}(T)]_{\mathrm{liquid}} V_{\mathrm{s}}}{Rt} \quad (2)$$

where V_{s} represents the volume of the suspension, R represents the air flow rate of the sampler, and t represents the collection time of the sample.

The corrected $[\mathrm{INP}(T)]_{\mathrm{liquid}}$ values were also used to calculate the number of INP per mass of aerosol particles ($n_{\mathrm{m}}(T)$) using the following equation:

$$n_{\mathrm{m}}(T) = \frac{[\mathrm{INP}(T)]_{\mathrm{liquid}}}{M_{\mathrm{s}}/V_{\mathrm{s}}} \quad (3)$$

where M_{s} represents the mass of aerosol particles in the suspension and V_{s} represents the volume of the suspension.

The number of INP per surface area of aerosol particles ($n_{\mathrm{s}}(T)$) was calculated using the equation below:

$$n_{\mathrm{s}}(T) = \frac{n_{\mathrm{m}}(T)}{S_{\mathrm{p}}/(\rho V_{\mathrm{p}})} \quad (4)$$

where S_{p} represents the total geometric surface area of particles in the suspensions, determined with the Coulter Counter, V_{p} represents the total geometric volume of particles in the suspensions, also determined with the Coulter Counter analysis, and ρ represents an assumed particle density of the aerosol particles (2.65 g cm^{-3}).[35] Eqn (4) assumes that the amount of water-soluble material in the collected samples was minor, which should be a reasonable assumption since the collected samples were most likely dominated by local mineral dust from glacial outwash sediments in the region (see below for details).

2.5. Heat assay and ammonium sulfate assay

Many proteinaceous INPs can be denatured by heat at 95 °C, resulting in a change in the tertiary structure of the proteinaceous INPs and a decrease in their ice nucleating ability.[36,37] In addition, previous studies have shown that the ice nucleating properties of mineral dusts such as K-feldspar, kaolinite, and montmorillonite barely change after heating.[36,38,39] Thus, a heating assay is a common method used to investigate the presence of biological INPs. In the current study, 1 mL of each suspension was heated at 100 °C for 1 hour in a sealed tube using an AccuBlock™ heating block. The heated suspensions were cooled down to room temperature, and then the ice nucleating property of the suspensions was measured using the droplet freezing technique. The difference between n_{m} values for heated and unheated samples was used to determine if the INPs were heat-sensitive and therefore, likely biological INPs.

The addition of ammonium sulfate at low concentrations (from 0.001 to 0.1 M) can increase the freezing temperatures of a variety of mineral INPs including feldspar, kaolinite, montmorillonite, quartz, and micas.[40–44] On the other hand, the freezing abilities of many biological INPs (*i.e.*, bacteria, fungi, diatom exudates, and leaf-derived materials) are not affected by the addition of ammonium sulfate at concentrations between 0.01 to 0.1 M, after correcting for freezing point depression.[40,45] Therefore, an ammonium sulfate assay has been suggested as a possible method to identify the presence of mineral dust INPs in atmospheric samples.[45] For the current study, 1 μL of ammonium sulfate solution with a concentration of 0.1 M was pipetted onto each droplet of glacial sample suspension to make 2 μL droplets containing 0.05 M ammonium sulfate. The ice nucleating property of the suspension after adding the ammonium sulfate solution was then measured using the droplet freezing technique discussed above. The freezing point depression (ΔT_{f}) caused by the ammonium sulfate was calculated using the equation below:

$$\Delta T_{\mathrm{f}} = iK_{\mathrm{f}} m_{\mathrm{solute}} \quad (5)$$

where i is the van't Hoff factor (3 for ammonium sulfate), K_{f} is the freezing point depression constant (1.86 °C kg mol^{-1} for water solution), and m_{solute} represents the molality of ammonium sulfate (0.05 mol kg^{-1}). ΔT_{f} was calculated to be 0.28 °C in our experiments, and all freezing temperatures were corrected for this ΔT_{f}. The difference between n_{m} values with and without the addition of ammonium sulfate, after correcting for freezing point depression, was used to determine if ice nucleation was dominated by ammonium sulfate-sensitive mineral dust INPs.

2.6. Predictions of mineral dust and INP concentrations using a global chemical transport model

We performed simulations using the GEOS-Chem chemical transport model (version 12.9.1, doi: **https://doi.org/10.5281/zenodo.3950473**)[46,47] to predict mineral dust concentrations during May 2018. Simulations of dust using GEOS-Chem have previously been found to be in good agreement with surface observations at Trapper Creek, Alaska spanning a full year[48] and CALIOP retrievals in the Arctic during the spring haze period.[49] GEOS-Chem is driven by assimilated meteorology from the Modern-Era Retrospective analysis for Research and

Applications, Version 2 (MERRA-2), at the NASA Global Modeling and Assimilation Office (GMAO). We generated boundary conditions using a global simulation at 2° latitude × 2.5° longitude resolution. We then used a nested grid with 0.5° latitude × 0.625° longitude resolution, spanning 40° N to 80° N, 180° W to 120° W. Our simulations included one month of spin-up. The atmosphere was resolved using 47 vertical layers from the surface to 0.01 hPa (about 100 m thick near the surface). We used the offline desert dust emissions described by Meng *et al.*,[50] which were in turn based on the Mineral Dust Entrainment and Deposition (DEAD) emissions scheme.[51] Notably, no natural high latitude dust emissions were included in the model.

In addition to determining mineral dust concentrations, we also determined the surface area of mineral dust from low latitude sources with the model. GEOS-Chem predicts mineral dust concentrations in the following bins: 0.1–1.0, 1.0–1.8, 1.8–3.0, and 3.0–6.0 μm. To determine the surface area of the mineral dust, we assumed that the dust particles had the middle radius of their bin. In addition, we assumed a mineral dust density of 2.5 g cm^{-3}. The mineral dust surface area simulated with the GEOS-Chem model was then used to predict INP concentrations, $[INP(T)]_{air}$, at the site by multiplying the surface area by an n_s parameterization from Ullrich *et al.* specifically developed for natural desert dust from low latitudes sources.[52]

3. Results and discussions

3.1. Concentration of INPs at the site

Listed in Table 1 and shown in Fig. 2a are the PM10 concentrations of the aerosol particles collected at the Down Valley site. Also included in Fig. 2a and b are the PM10 concentrations of the aerosols at the nearby Visitor's Center site (location shown in Fig. 1), and the vertical flux of aerosol particles at the Down Valley site, based on previous measurements. On the days that filter samples were collected at the Down Valley site for freezing measurements, the PM10 aerosol concentrations ranged from approximately 100 to 1400 μg m^{-3}. Several pieces of evidence suggest that the aerosol particles sampled on these days were dominated by local mineral dust from glacial outwash sediments in the region. First, all the days that filter samples were collected correspond to extreme dust events if we use the 24 h average WHO health standard for PM10 (50 μg m^{-3}) as the criteria for an extreme dust event, as done previously (Fig. 2a).[53,54] Second, the mass concentrations at the Down Valley site were substantially higher than those at the nearby Visitor's Center site for all days except one (Fig. 2a), suggesting a local dust source near the Down Valley site. Note, the Down Valley site was near the center of the exposed A'äy Chù Delta, whereas the Visitor's Center site was off to the side of the exposed delta (Fig. 1). Third, the vertical aerosol flux at the Down Valley site was positive for all of the days that samples were collected and vertical aerosol flux measurements were made (Fig. 2b), confirming that the glacial outwash sediments were an emission source at the Down Valley site for these days. Fourth, only mineral dust particles were detected in samples

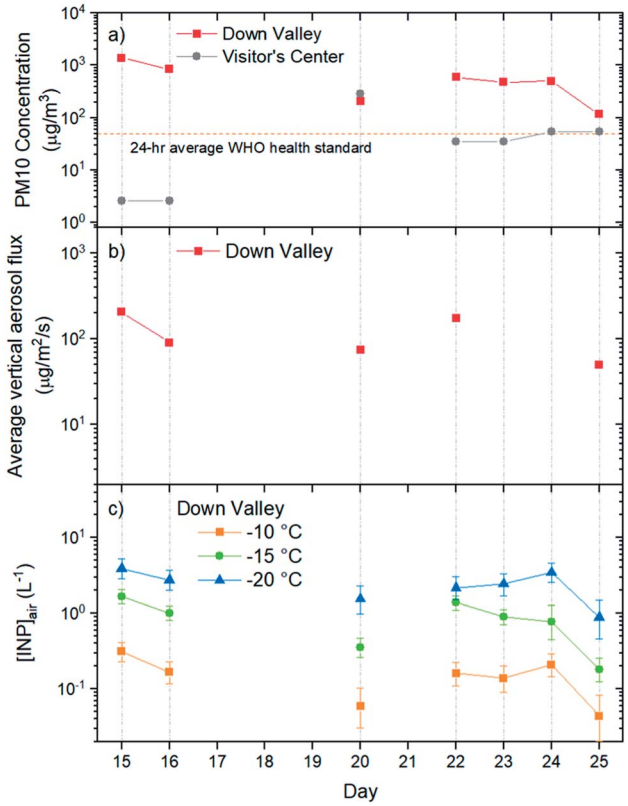

Fig. 2 (a) PM10 mass concentrations at the Down Valley site and nearby Visitor's Center site on days when samples were collected for INP measurements. Included is the 24 h average WHO health standard for PM10 concentrations. (b) The average vertical aerosol flux at the Down Valley site for the days vertical aerosol flux measurements were made and INP samples were collected. (c) Numbers of INPs per volume of air at the Down Valley site for freezing temperatures of −10, −15, and −20 °C.

collected from the Down Valley site during the same month and year and for similar PM10 levels (but on a different day) based on SEM/EDX measurements, with the caveat that carbonaceous or semi-volatile materials could not be detected with the SEM/EDX measurements. For details of PM10 measurements at the Visitor's Center site, vertical aerosol flux measurements at the Down Valley site, and the SEM/EDX measurements at the Down Valley site, see Bachelder *et al.*[23]

Shown in Fig. 3 are freezing curves for the samples collected at the Down Valley site. The samples caused freezing at temperatures ranging from −6 to −23 °C, which is considerably warmer than that of the lab blanks and the field blanks (Fig. 3), indicating the samples contained effective INPs.

Based on the freezing results, the concentration of INPs in the air at the sampling site ($[INP]_{air}$) ranged from 5×10^{-3} to 2×10^{1} L^{-1} at freezing temperatures ranging from −6 to −23 °C (Fig. 4). These values are at the upper end of values previously measured over North America and Europe and are above values previously measured at high latitudes over the Arctic (Fig. 4).

On the days filter samples were collected, the INP concentrations at the site were correlated with the PM10 concentrations of the aerosols at the site (compare Fig. 2a and c).

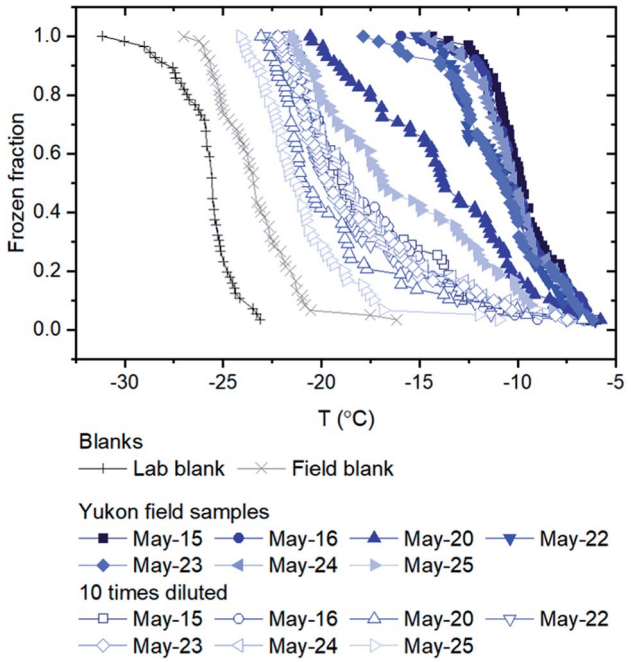

Fig. 3 Frozen fractions of droplets for blanks (both lab blanks and field blanks) and suspensions of Yukon field samples. Lab blanks correspond to MilliQ water and field blanks correspond to a filter not exposed to aerosols, but treated with the same process as the field samples. The uncertainty in the temperature measurement (±0.25 °C) was not included as the uncertainty of the measurement was similar to the symbol sizes.

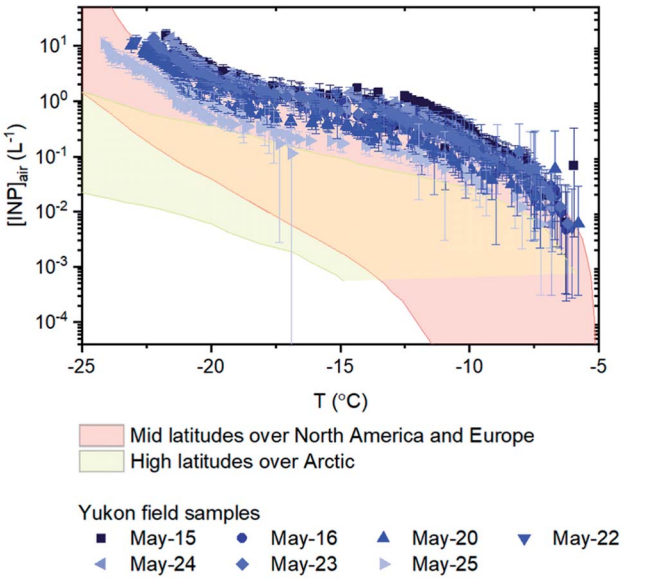

Fig. 4 Numbers of INPs per volume of air for the sampling days. Included for comparison purposes are concentrations measured at mid latitudes over North America and Europe (pink shading)[69] and concentrations measured at high latitudes over the Arctic (yellow shading).[7–14,70–75] The $[INP]_{air}$ values used to estimate concentrations measured at high latitudes over the Arctic are shown in Fig. S2.† Error bars for the field samples were calculated based on 95% confidence intervals from nucleation statistics.[76]

Correlation coefficients (R^2) were 0.88, 0.80, and 0.70, and p-values were 0.003, 0.007, and 0.019 for freezing temperatures of −10, −15, and −20 °C, respectively. The correlation between the concentration of INPs and PM10 concentrations is consistent with the aerosol particles collected at the Down Valley site being dominated by mineral dust from glacial outwash sediments in the region.

3.2. Ice nucleating abilities of the glacier samples

3.2.1. n_m values of the glacier samples. The number of INPs per mass of material, n_m, for the glacial dust samples ranged from 6×10^3 to 3×10^7 g^{-1} at temperatures from −6 to −23 °C (Fig. 5). The n_m values for the glacial dust samples from different days were similar (within one order of magnitude), suggesting that the freezing properties of the glacial dust did not change drastically from day-to-day. A polynomial was fit to the n_m data (Fig. 5, solid line), which can be used for predicting concentrations of INPs at the site (see below).

The n_m values of the airborne dust in the current study were two orders of magnitude lower than that of the glacial outwash sediments from Svalbard obtained by Tobo *et al.* (Fig. 5), indicating that the airborne dust from the Kaskawulsh Glacier in Yukon, Canada was less effective at nucleating ice than the surface-collected glacial outwash sediments from Svalbard.[18] The high n_m values associated with the glacial outwash sediments from Svalbard were likely due to a small amount of organic material present in the sediments that was highly effective at nucleating ice based on a hydrogen peroxide assay.[18] The difference in the results between the current aerosol samples and the Svalbard glacial outwash sediments may be because the Yukon glacial outwash sediments contain less organic material that is highly effective at nucleating ice. Alternatively, the Yukon glacial outwash sediments may contain organic material that is highly effective at nucleating ice, but the organic material was not effectively aerosolized at the Yukon site. In addition, the Yukon glacial outwash sediments may have a different mineralogy than the samples collected from Svalbard. Measurements of the amount of organic material in the airborne dust at the Yukon site, as well as the ice nucleating ability of surface-collected glacier outwash sediments at the Yukon site, would be useful to understand these differences. A comparison of the mineralogy at the two sites would also be helpful.

Also included in Fig. 5 are n_m values for the active layer (samples collected 0.15 m below the surface) from Fairbanks, Alaska, USA during August 2019.[55] The n_m values of the airborne dust in the current study was also approximately 0–2 orders of magnitude lower than those of the active layer collected from Alaska. Several reasons could explain these differences. For example, the differences could be due to differences between aerosolized samples and samples collected below the surface. The differences could also be due to differences in mineralogy and biology at the Yukon site compared to the Fairbanks site, such as different microclimates and different mineral formation mechanisms between the two regions.

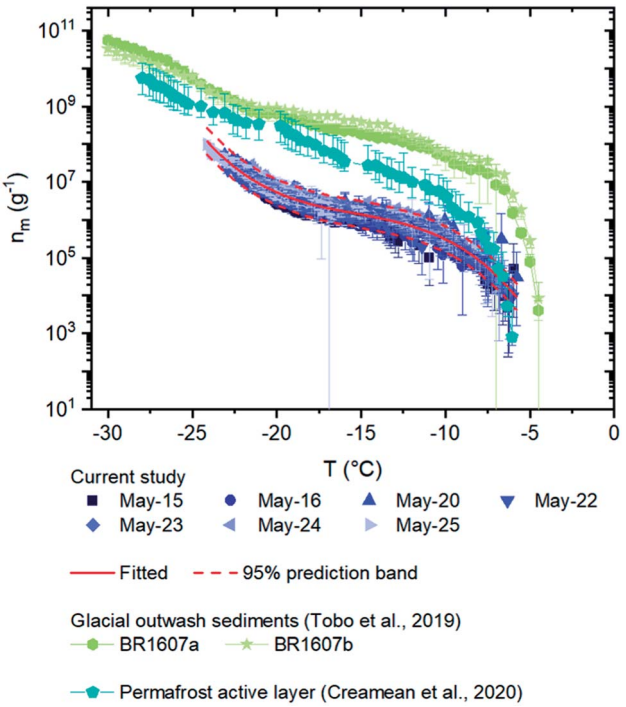

Fig. 5 Numbers of INPs per mass of materials (n_m) for the field samples. Error bars for the field samples were calculated based on 95% confidence intervals from nucleation statistics.[76] The solid curve and the dashed curves correspond to a fitted line: $n_m(T) = \exp(-2.57904 - 2.93411T - 0.180657T^2 - 0.003957T^3)$ with T ranging from −6 to −23 °C, and the 95% prediction band from the fit. The n_m values of surface-collected glacial outwash sediments obtained in Svalbard and a permafrost active layer collected in Fairbanks are plotted for comparison.[18,55]

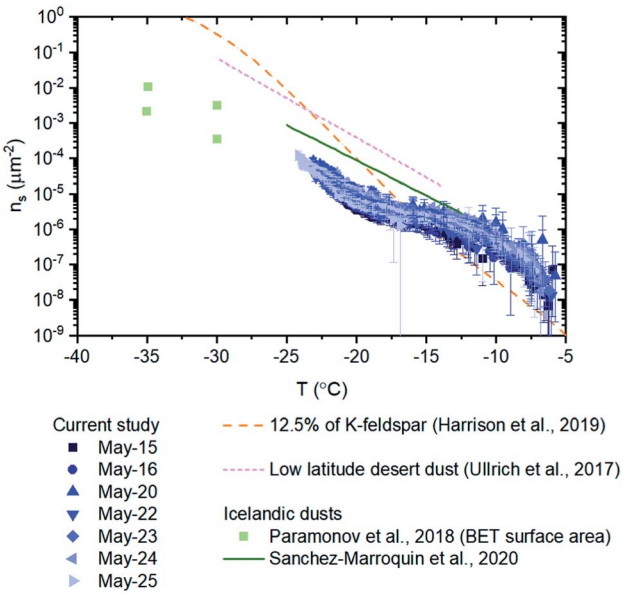

Fig. 6 Numbers of INPs per surface area of material (n_s) for field samples. Error bars for the field samples were calculated based on 95% confidence intervals from nucleation statistics (Koop *et al.*, 1997) and the uncertainty (two standard deviations based on triplicate runs) in the surface area measurements. The n_s-values of 12.5% of K-feldspar, low latitude desert dust, and Icelandic dust are also plotted for comparison.[19,22,52,63] The n_s data from Paramonov *et al.* and Harrison *et al.* are based on BET surface areas, while all of the other data is based on geometric surface areas. The $n_{s,\ BET}$ data of K-feldspar was converted to $n_{s,\ geo}$ data using a normalization factor of 2.6/0.89.[77]

3.2.2. n_s values of the glacier samples. The size distributions of the particles in the glacial dust suspensions used in the freezing measurements were similar for all seven days, with the maximum count fraction of surface areas between 2 and 5 μm (Fig. S1†). The surface area distributions of the suspensions were used to determine the number of INPs per surface area of the glacial dust (eqn (4)). The n_s values ranged from 8×10^{-9} to 1×10^{-4} μm^{-2} at freezing temperatures from −6 to −23 °C (Fig. 6). Similar to the n_m values, the n_s values for the glacial dust samples changed by less than one order of magnitude from day-to-day. The n_s values of the glacial dust samples were compared with n_s values of K-feldspar, which is considered one of the most active ice nucleating minerals[39,56–60] and is a major atmospheric INP based on field measurements and modelling studies.[60–62] According to the mineralogical classification conducted by Bachelder *et al.* using SEM/EDS on samples collected from the same site during the same time period, around 25% of particles in the glacial dust samples were feldspar.[23] A reanalysis of dust samples collected from the site suggests that the feldspar in the samples consisted of approximately 50% plagioclase and 50% orthoclase (also referred to as K-feldspar) (Text S1†). As a result, we assumed that 12.5% of the surface area of the particles was K-feldspar. The n_s value for K-feldspar[63] multiplied by 0.125 is included in Fig. 6 for comparison. The n_s values for K-feldspar multiplied by 0.125 are similar to the n_s values for our samples at temperatures between approximately −15 to −17 °C, but are lower at warmer temperatures and higher at colder temperatures. This difference suggests that the ice nucleating ability of the glacial dust samples cannot be explained by K-feldspar alone at temperatures warmer than −15 °C.

The n_s values of the glacial dust samples were also compared with parameterizations of n_s values for low latitude desert dust from Ullrich *et al.* (Fig. 6). Low latitude desert dust is an important source of atmospheric INPs due to their abundance in the atmosphere and their high efficiency in ice nucleation.[52,62,64,65] The n_s values for desert dust are around 1–2 orders of magnitude higher than that of the glacial dust samples at temperatures colder than −15 °C.[52] We also compared our n_s values with n_s values of airborne Icelandic dust[19] and n_s values of glaciogenic silt collected from a glacial river in Iceland[22] (Fig. 6). The n_s values of the airborne Icelandic dust are around one order of magnitude higher than the n_s values from our studies at temperatures less than −15 °C. The n_s values of the glaciogenic silt were determined for lower temperatures than measured here, so a direct comparison is not possible.

3.2.3. INP composition of the glacial samples. To provide additional insight on the composition of the INPs, we carried out a heat assay and an ammonium sulfate assay (Fig. 7). In our study, the presence of ammonium sulfate caused almost no change to the freezing properties of the samples at freezing

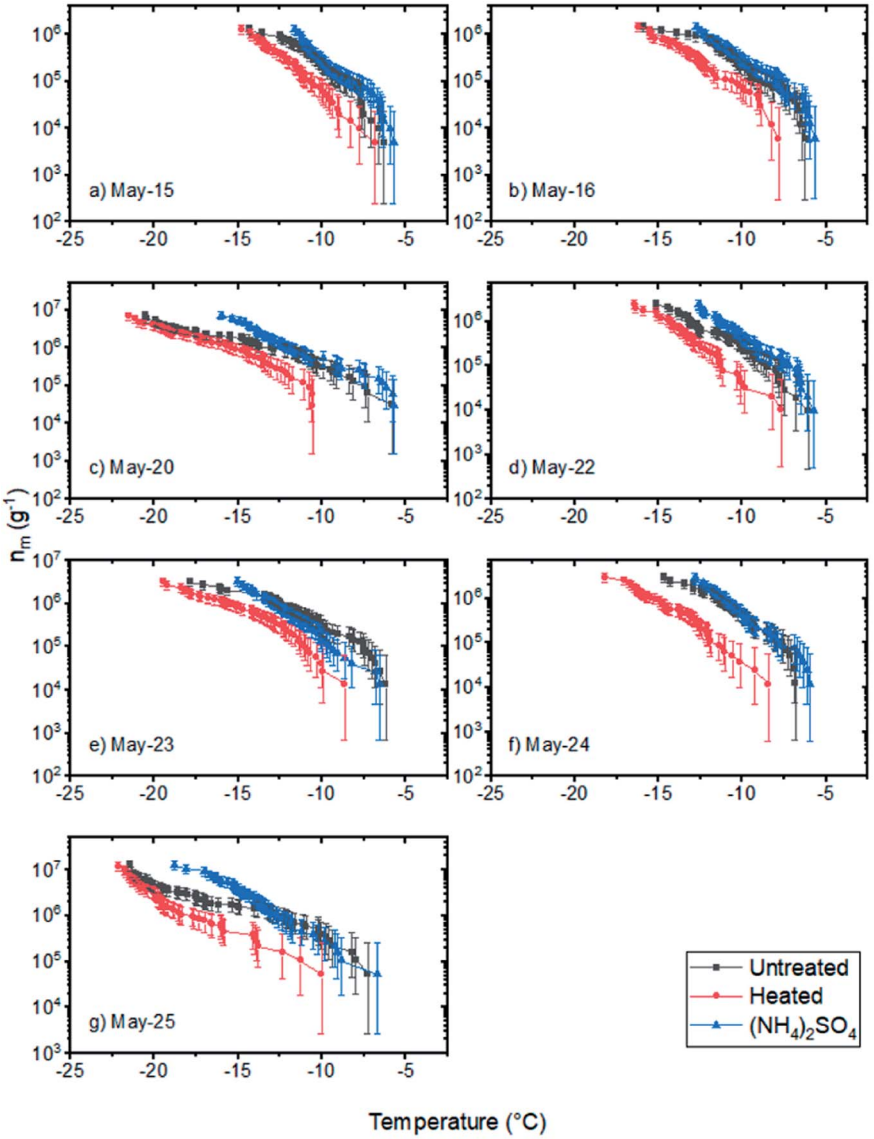

Fig. 7 Numbers of INPs per mass of field samples (n_m) without treatment, after heating to 100 °C for 1 hour, and after the addition of ammonium sulfate (0.05 M) (a–g). Error bars for the samples were calculated based on 95% confidence intervals from nucleation statistics.[76]

temperatures warmer than −15 °C. The results from the ammonium sulfate tests suggest that K-feldspar or quartz, which are major components of the airborne dust according to the analysis conducted by Bachelder *et al.*, are not the main components controlling the ice nucleating ability of the glacial dust samples at freezing temperatures above −15 °C. This is consistent with the n_s results (Fig. 6) which show that the n_s of the glacial dust samples is higher than 12.5% of the n_s values of K-feldspar at temperatures warmer than −15 °C.

In the heat tests, we observed that the n_m values at freezing temperatures warmer than −15 °C for all of the samples decreased by a factor of 2 to 10 after being heated at 100 °C. These results, combined with the fact that the ammonium sulfate assay caused almost no change in the n_m values at freezing temperatures warmer than −15 °C suggests that the INPs that caused freezing at temperatures warmer than −15 °C were biological and likely proteinaceous. Biological materials, which are rich in glacier ecosystems, can be transported by meltwater and deposited in outwash sediments.[66–68] Consistent with these results, Tobo *et al.* attributed the high ice nucleating ability of their glacial outwash sediments collected in Svalbard to biological activity.[18]

3.3. INP concentrations at the site for May 2018

Although we only measured INP concentrations at the site during seven days in May 2018, we can estimate INP concentrations at the site for most of the month of May using our new n_m parameterization (Fig. 5) and PM10 measurements at the site from May 10th to May 29th 2018 (Fig. 8). The predicted average $[INP]_{air}$ values using this approach ranged from 9×10^{-3} to 3×10^{1} L^{-1} at temperatures from −6 to −23 °C (Fig. 9). The predicted average $[INP]_{air}$ values were at the upper end of

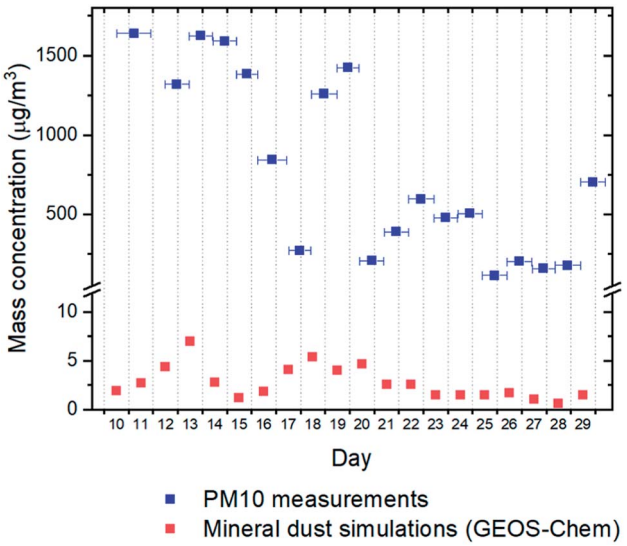

Fig. 8 Comparison of PM10 mass concentrations determined from gravimetric analysis of collected Nuclepore filters previously reported in the literature[23] and mineral dust concentrations predictions using GEOS-Chem for May 10th to May 29th 2018 from low latitude sources. The horizontal error bars for the field measurements correspond to the range of sampling times for the filter samples.

values previously measured over North America and Europe and are well above values previously measured at high latitudes over the Arctic.

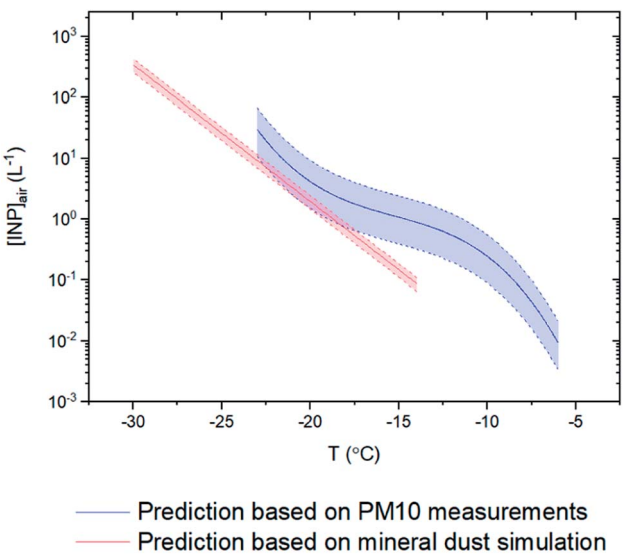

Fig. 9 Prediction curves for the average numbers of INPs per volume of air ($[INP]_{air}$) from May 10th to May 29th 2018. The blue curve corresponds to predictions using measured PM10 concentrations at the site (Fig. 8) and the n_m parameterization for the glacier dust samples determined here (Fig. 5). The red curve corresponds to predictions using simulated surface areas of natural mineral dust at the site from low latitude sources using GEOS-Chem and an n_s parameterization from Ullrich *et al.*[52] Error bars are based on the 95% confidence level of mineral dust mass/surface area from the filters/simulations from May 10th to May 29th and the 95% confidence level in the n_m parameterization for the glacier dust samples.

For comparison purposes, we also predicted the average $[INP]_{air}$ concentrations at the site for the same time period using simulated natural mineral dust surface areas at the site from low latitude sources using GEOS-Chem and an n_s parameterization from Ullrich *et al.*[52] The dust concentrations predicted with GEOS-Chem were more than two orders of magnitude lower than the dust concentrations measured at the site (Fig. 8). This under-prediction of dust concentrations led to an under-prediction of average $[INP]_{air}$ values by around one order of magnitude at −15 °C compared to the values estimated using the average measured PM10 concentrations (Fig. 9).

4. Summary and conclusion

The ice nucleating properties of aerosol particles collected near the Kaskawulsh Glacier, an actively retreating glacier in Yukon, Canada, during May 2018 were investigated. Several pieces of evidence suggest that the aerosol particles sampled on these days were dominated by local mineral dust from glacial outwash sediments in the region. The airborne dust caused freezing from −6 to −23 °C, suggesting that effective INPs were present in the glacial dust. The atmospheric INP concentrations were at the upper range of values previously measured over continental North America and Europe and were higher than the values previously measured at high latitudes over the Arctic.

The ice nucleating ability of the glacial dust was significantly worse than the ice nucleating ability of glacial outwash sediments collected in Svalbard based on a comparison of n_m values. This difference may be due to differences between aerosolized samples and surface-collected samples or differences in mineralogy and biology between the two sites.

A heat assay and an ammonium sulfate assay were conducted on the airborne glacial dust samples at freezing temperatures greater than −15 °C. The decrease in the ice nucleating ability after heating and the lack of change in the ice nucleating ability after the addition of ammonium sulfate suggest that the INPs at freezing temperatures greater than −15 °C may be biological. This conclusion agrees with the comparison of n_s values between the glacial dust samples and K-feldspar.

Based our n_m parameterization for the airborne glacial dust at the site and PM10 measurements at the site from May 10th to May 29th 2018, the average $[INP]_{air}$ values at the site for this time period ranged from 9×10^{-3} to 3×10^{1} L^{-1} at freezing temperatures from −6 to −23 °C. These concentrations, at a freezing temperature of −15 °C, were approximately one order of magnitude higher than predictions based on simulations with the GEOS-Chem model and only considering low latitude natural dust sources. This difference in concentrations illustrates that the inclusion of high latitude natural dust sources is needed for predicting INP concentrations at the site.

Conflicts of interest

There is no conflict to declare.

Acknowledgements

We respectively acknowledge that the sample collection and field work were performed on the traditional territories of the Kluane First Nation and the Champagne and Aishihik First Nations. A. K. B, Y. X., and C. X. acknowledge funding from the Natural Sciences and Engineering Research Council of Canada (NSERC) Discovery Grants program. A. D., R. S., J. O. B., P. L. H, and J. K. acknowledge funding support from the NSERC Discovery Grants program, CFI, and the Canadian Mountain Network (a Canadian Government Network of Centers of Excellence). The GEOS-Chem modeling was enabled in part by support provided by Calcul Québec and Compute Canada.

References

1 Z. A. Kanji, L. A. Ladino, H. Wex, Y. Boose, M. Burkert-Kohn, D. J. Cziczo and M. Krämer, Overview of Ice Nucleating Particles, *Meteorol. Monogr.*, 2017, **58**, 1–33.

2 B. J. Murray, D. O'Sullivan, J. D. Atkinson and M. E. Webb, Ice nucleation by particles immersed in supercooled cloud droplets, *Chem. Soc. Rev.*, 2012, **41**, 6519.

3 T. Storelvmo, Aerosol Effects on Climate via Mixed-Phase and Ice Clouds, *Annu. Rev. Earth Planet. Sci.*, 2017, **45**, 199–222.

4 P. J. DeMott, A. J. Prenni, X. Liu, S. M. Kreidenweis, M. D. Petters, C. H. Twohy, M. S. Richardson, T. Eidhammer and D. C. Rogers, Predicting global atmospheric ice nuclei distributions and their impacts on climate, *Proc. Natl. Acad. Sci. U.S.A.*, 2010, **107**, 11217–11222.

5 U. Lohmann and J. Feichter, Global indirect aerosol effects: a review, *Atmos. Chem. Phys.*, 2005, **5**, 715–737.

6 J. Fan, L. R. Leung, D. Rosenfeld and P. J. DeMott, Effects of cloud condensation nuclei and ice nucleating particles on precipitation processes and supercooled liquid in mixed-phase orographic clouds, *Atmos. Chem. Phys.*, 2017, **17**, 1017–1035.

7 V. E. Irish, S. J. Hanna, Y. Xi, M. Boyer, E. Polishchuk, M. Ahmed, J. Chen, J. P. D. Abbatt, M. Gosselin, R. Chang, L. A. Miller and A. K. Bertram, Revisiting properties and concentrations of ice-nucleating particles in the sea surface microlayer and bulk seawater in the Canadian Arctic during summer, *Atmos. Chem. Phys.*, 2019, **19**, 7775–7787.

8 T. Šantl-Temkiv, R. Lange, D. Beddows, U. Rauter, S. Pilgaard, M. Dall'Osto, N. Gunde-Cimerman, A. Massling and H. Wex, Biogenic Sources of Ice Nucleating Particles at the High Arctic Site Villum Research Station, *Environ. Sci. Technol.*, 2019, **53**, 10580–10590.

9 H. Wex, L. Huang, W. Zhang, H. Hung, R. Traversi, S. Becagli, R. J. Sheesley, C. E. Moffett, T. E. Barrett, R. Bossi, H. Skov, A. Hünerbein, J. Lubitz, M. Löffler, O. Linke, M. Hartmann, P. Herenz and F. Stratmann, Annual variability of ice-nucleating particle concentrations at different Arctic locations, *Atmos. Chem. Phys.*, 2019, **19**, 5293–5311.

10 J. M. Creamean, R. M. Kirpes, K. A. Pratt, N. J. Spada, M. Maahn, G. de Boer, R. C. Schnell and S. China, Marine and terrestrial influences on ice nucleating particles during continuous springtime measurements in an Arctic oilfield location, *Atmos. Chem. Phys.*, 2018, **18**, 18023–18042.

11 J. M. Creamean, J. N. Cross, R. Pickart, L. McRaven, P. Lin, A. Pacini, R. Hanlon, D. G. Schmale, J. Ceniceros, T. Aydell, N. Colombi, E. Bolger and P. J. DeMott, Ice Nucleating Particles Carried From Below a Phytoplankton Bloom to the Arctic Atmosphere, *Geophys. Res. Lett.*, 2019, **46**, 8572–8581.

12 A. Welti, E. K. Bigg, P. J. DeMott, X. Gong, M. Hartmann, M. Harvey, S. Henning, P. Herenz, T. C. J. Hill, B. Hornblow, C. Leck, M. Löffler, C. S. McCluskey, A. M. Rauker, J. Schmale, C. Tatzelt, M. van Pinxteren and F. Stratmann, Ship-based measurements of ice nuclei concentrations over the Arctic, Atlantic, Pacific and Southern oceans, *Atmos. Chem. Phys.*, 2020, **20**, 15191–15206.

13 M. Hartmann, K. Adachi, O. Eppers, C. Haas, A. Herber, R. Holzinger, A. Hünerbein, E. Jäkel, C. Jentzsch, M. Pinxteren, H. Wex, S. Willmes and F. Stratmann, Wintertime Airborne Measurements of Ice Nucleating Particles in the High Arctic: A Hint to a Marine, Biogenic Source for Ice Nucleating Particles, *Geophys. Res. Lett.*, 2020, **47**, 1–11.

14 M. Si, E. Evoy, J. Yun, Y. Xi, S. J. Hanna, A. Chivulescu, K. Rawlings, D. Veber, A. Platt, D. Kunkel, P. Hoor, S. Sharma, W. Richard Leaitch and A. K. Bertram, Concentrations, composition, and sources of ice-nucleating particles in the Canadian High Arctic during spring 2016, *Atmos. Chem. Phys.*, 2019, **19**, 3007–3024.

15 B. J. Murray, K. S. Carslaw and P. R. Field, Opinion: Cloud-phase climate feedback and the importance of ice-nucleating particles, *Atmos. Chem. Phys.*, 2021, **21**, 665–679.

16 M. D. Shupe, Clouds at Arctic Atmospheric Observatories. Part II: Thermodynamic Phase Characteristics, *J. Appl. Meteorol. Climatol.*, 2011, **50**, 645–661.

17 2013 IPCC, *Climate Change 2013: the Physical Science Basis. Contribution of Working Group I to the Fifth Assessment Report of the Intergovernmental Panel on Climate Change*, Cambridge University Press, Cambridge, United Kingdom and New York, NY, USA, 2013.

18 Y. Tobo, K. Adachi, P. J. DeMott, T. C. J. Hill, D. S. Hamilton, N. M. Mahowald, N. Nagatsuka, S. Ohata, J. Uetake, Y. Kondo and M. Koike, Glacially sourced dust as a potentially significant source of ice nucleating particles, *Nat. Geosci.*, 2019, **12**, 253–258.

19 A. Sanchez-Marroquin, O. Arnalds, K. J. Baustian-Dorsi, J. Browse, P. Dagsson-Waldhauserova, A. D. Harrison, E. C. Maters, K. J. Pringle, J. Vergara-Temprado, I. T. Burke, J. B. McQuaid, K. S. Carslaw and B. J. Murray, Iceland is an episodic source of atmospheric ice-nucleating particles relevant for mixed-phase clouds, *Sci. Adv.*, 2020, **6**, eaba8137.

20 J. E. Bullard, Contemporary glacigenic inputs to the dust cycle, *Earth Surf. Process. Landforms*, 2013, **38**, 71–89.

21 J. E. Bullard, M. Baddock, T. Bradwell, J. Crusius, E. Darlington, D. Gaiero, S. Gassó, G. Gisladottir, R. Hodgkins, R. McCulloch, C. McKenna-Neuman, T. Mockford, H. Stewart and T. Thorsteinsson,

High-latitude dust in the Earth system, *Rev. Geophys.*, 2016, **54**, 447–485.

22 M. Paramonov, R. O. David, R. Kretzschmar and Z. A. Kanji, A laboratory investigation of the ice nucleation efficiency of three types of mineral and soil dust, *Atmos. Chem. Phys.*, 2018, **18**, 16515–16536.

23 J. Bachelder, M. Cadieux, C. Liu-Kang, P. Lambert, A. Filoche, J. A. Galhardi, M. Hadioui, A. Chaput, M.-P. Bastien-Thibault, K. J. Wilkinson, J. King and P. L. Hayes, Chemical and microphysical properties of wind-blown dust near an actively retreating glacier in Yukon, Canada, *Aerosol Sci. Technol.*, 2020, **54**, 2–20.

24 W. G. Nickling, Eolian sediment transport during dust storms: Slims River Valley, Yukon Territory, *Can. J. Earth Sci.*, 1978, **15**, 1069–1084.

25 D. H. Shugar, J. J. Clague, J. L. Best, C. Schoof, M. J. Willis, L. Copland and G. H. Roe, River piracy and drainage basin reorganization led by climate-driven glacier retreat, *Nat. Geosci.*, 2017, **10**, 370–375.

26 P. J. DeMott, T. C. J. Hill, M. D. Petters, A. K. Bertram, Y. Tobo, R. H. Mason, K. J. Suski, C. S. McCluskey, E. J. T. Levin, G. P. Schill, Y. Boose, A. M. Rauker, A. J. Miller, J. Zaragoza, K. Rocci, N. E. Rothfuss, H. P. Taylor, J. D. Hader, C. Chou, J. A. Huffman, U. Pöschl, A. J. Prenni and S. M. Kreidenweis, Comparative measurements of ambient atmospheric concentrations of ice nucleating particles using multiple immersion freezing methods and a continuous flow diffusion chamber, *Atmos. Chem. Phys. Discuss.*, 2017, **17**, 11227–11245.

27 R. W. DeBlois and C. P. Bean, Counting and Sizing of Submicron Particles by the Resistive Pulse Technique, *Rev. Sci. Instrum.*, 1970, **41**, 909–916.

28 T. F. Whale, B. J. Murray, D. O'Sullivan, T. W. Wilson, N. S. Umo, K. J. Baustian, J. D. Atkinson, D. A. Workneh and G. J. Morris, A technique for quantifying heterogeneous ice nucleation in microlitre supercooled water droplets, *Atmos. Meas. Tech.*, 2015, **8**, 2437–2447.

29 V. E. Irish, P. Elizondo, J. Chen, C. Choul, J. Charette, M. Lizotte, L. A. Ladino, T. W. Wilson, M. Gosselin, B. J. Murray, E. Polishchuk, J. P. D. Abbatt, L. A. Miller and A. K. Bertram, Ice-nucleating particles in Canadian Arctic sea-surface microlayer and bulk seawater, *Atmos. Chem. Phys.*, 2017, **17**, 10583–10595.

30 J. Yun, A. Kumar, N. Removski, A. Shchukarev, N. Link, J.-F. Boily and A. K. Bertram, Effects of Inorganic Acids and Organic Solutes on the Ice Nucleating Ability and Surface Properties of Potassium-Rich Feldspar, *ACS Earth Sp. Chem.*, 2021, **5**, 1212–1222.

31 Y. Xi, A. Mercier, C. Kuang, J. Yun, A. Christy, L. Melo, M. T. Maldonado, J. A. Raymond and A. K. Bertram, Concentrations and properties of ice nucleating substances in exudates from Antarctic sea-ice diatoms, *Environ. Sci. Process. Impacts*, 2021, **23**, 323–334.

32 R. D. Lide, *CRC Handbook of Chemistry and Physics*, CRC Press LLC, Boca Raton, 82nd edn, 2001.

33 T. W. Wilson, L. A. Ladino, P. A. Alpert, M. N. Breckels, I. M. Brooks, J. Browse, S. M. Burrows, K. S. Carslaw, J. A. Huffman, C. Judd, W. P. Kilthau, R. H. Mason, G. McFiggans, L. A. Miller, J. J. Najera, E. Polishchuk, S. Rae, C. L. Schiller, M. Si, J. V. Temprado, T. F. Whale, J. P. S. Wong, O. Wurl, J. D. Yakobi-Hancock, J. P. D. Abbatt, J. Y. Aller, A. K. Bertram, D. A. Knopf and B. J. Murray, A marine biogenic source of atmospheric ice-nucleating particles, *Nature*, 2015, **525**, 234–238.

34 G. Vali, Quantitative Evaluation of Experimental Results an the Heterogeneous Freezing Nucleation of Supercooled Liquids, *J. Atmos. Sci.*, 1971, **28**, 402–409.

35 Y. H. Lee, K. Chen and P. J. Adams, Development of a global model of mineral dust aerosol microphysics, *Atmos. Chem. Phys.*, 2009, **9**, 2441–2458.

36 T. C. J. Hill, P. J. DeMott, Y. Tobo, J. Fröhlich-Nowoisky, B. F. Moffett, G. D. Franc and S. M. Kreidenweis, Sources of organic ice nucleating particles in soils, *Atmos. Chem. Phys.*, 2016, **16**, 7195–7211.

37 B. C. Christner, R. Cai, C. E. Morris, K. S. McCarter, C. M. Foreman, M. L. Skidmore, S. N. Montross and D. C. Sands, Geographic, seasonal, and precipitation chemistry influence on the abundance and activity of biological ice nucleators in rain and snow, *Proc. Natl. Acad. Sci. U.S.A.*, 2008, **105**, 18854–18859.

38 F. Conen, C. E. Morris, J. Leifeld, M. V. Yakutin and C. Alewell, Biological residues define the ice nucleation properties of soil dust, *Atmos. Chem. Phys.*, 2011, **11**, 9643–9648.

39 A. Peckhaus, A. Kiselev, T. Hiron, M. Ebert and T. Leisner, A comparative study of K-rich and Na/Ca-rich feldspar ice-nucleating particles in a nanoliter droplet freezing assay, *Atmos. Chem. Phys.*, 2016, **16**, 11477–11496.

40 M. T. Reischel and G. Vali, Freezing nucleation in aqueous electrolytes, *Tellus*, 1975, **27**, 414–427.

41 T. F. Whale, M. A. Holden, T. W. Wilson, D. O'Sullivan and B. J. Murray, The enhancement and suppression of immersion mode heterogeneous ice-nucleation by solutes, *Chem. Sci.*, 2018, **9**, 4142–4151.

42 R. J. Perkins, S. M. Gillette, T. C. J. Hill and P. J. DeMott, The Labile Nature of Ice Nucleation by Arizona Test Dust, *ACS Earth Sp. Chem.*, 2020, **4**, 133–141.

43 A. Kumar, C. Marcolli, B. Luo and T. Peter, Ice nucleation activity of silicates and aluminosilicates in pure water and aqueous solutions – Part 1: The K-feldspar microcline, *Atmos. Chem. Phys.*, 2018, **18**, 7057–7079.

44 A. Kumar, C. Marcolli and T. Peter, Ice nucleation activity of silicates and aluminosilicates in pure water and aqueous solutions – Part 2: Quartz and amorphous silica, *Atmos. Chem. Phys.*, 2019, **19**, 6035–6058.

45 S. Worthy, A. Kumar, Y. Xi, J. Yun, J. Chen, C. Xu, V. Irish, P. Amato and A. Bertram, The effect of (NH4)2SO4 on the freezing properties of non-mineral dust ice nucleating substances of atmospheric relevance, *Atmos. Chem. Phys. Discuss.*, 2021, 1–30.

46 I. Bey, D. J. Jacob, R. M. Yantosca, J. A. Logan, B. D. Field, A. M. Fiore, Q. Li, H. Y. Liu, L. J. Mickley and M. G. Schultz, *J. Geophys. Res. Atmos.*, 2001, **106**, 23073–23095.

47 R. J. Park, D. J. Jacob, B. D. Field, R. M. Yantosca and M. Chin, Natural and transboundary pollution influences on sulfate-nitrate-ammonium aerosols in the United States: Implications for policy, *J. Geophys. Res.*, 2004, **109**, D15204.

48 T. J. Breider, L. J. Mickley, D. J. Jacob, Q. Wang, J. A. Fisher, R. Y.-W. Chang and B. Alexander, Annual distributions and sources of Arctic aerosol components, aerosol optical depth, and aerosol absorption, *J. Geophys. Res. Atmos.*, 2014, **119**, 4107–4124.

49 M. Di Pierro, L. Jaeglé and T. L. Anderson, Satellite observations of aerosol transport from East Asia to the Arctic: three case studies, *Atmos. Chem. Phys.*, 2011, **11**, 2225–2243.

50 J. Meng, R. V Martin, P. Ginoux, M. Hammer, M. P. Sulprizio, D. A. Ridley and A. van Donkelaar, Grid-independent high-resolution dust emissions (v1.0) for chemical transport models: application to GEOS-Chem (12.5.0), *Geosci. Model Dev.*, 2021, **14**, 4249–4260.

51 C. S. Zender, H. Bian and D. Newman, Mineral Dust Entrainment and Deposition (DEAD) model: Description and 1990s dust climatology, *J. Geophys. Res.*, 2003, **108**, 4416.

52 R. Ullrich, C. Hoose, O. Möhler, M. Niemand, R. Wagner, K. Höhler, N. Hiranuma, H. Saathoff and T. Leisner, A New Ice Nucleation Active Site Parameterization for Desert Dust and Soot, *J. Atmos. Sci.*, 2017, **74**, 699–717.

53 H. Gandham, H. P. Dasari, S. Langodan, R. K. Karumuri and I. Hoteit, Major Changes in Extreme Dust Events Dynamics Over the Arabian Peninsula During 2003–2017 Driven by Atmospheric Conditions, *J. Geophys. Res. Atmos.*, 2020, **125**, e2020JD032931.

54 Y. O. Khaniabadi, S. M. Daryanoosh, A. Amrane, R. Polosa, P. K. Hopke, G. Goudarzi, M. J. Mohammadi, P. Sicard and H. Armin, Impact of Middle Eastern Dust storms on human health, *Atmos. Pollut. Res.*, 2017, **8**, 606–613.

55 J. M. Creamean, T. C. J. Hill, P. J. DeMott, J. Uetake, S. Kreidenweis and T. A. Douglas, Thawing permafrost: an overlooked source of seeds for Arctic cloud formation, *Environ. Res. Lett.*, 2020, **15**, 084022.

56 S. Augustin-Bauditz, H. Wex, S. Kanter, M. Ebert, D. Niedermeier, F. Stolz, A. Prager and F. Stratmann, The immersion mode ice nucleation behavior of mineral dusts: A comparison of different pure and surface modified dusts, *Geophys. Res. Lett.*, 2014, **41**, 7375–7382.

57 A. D. Harrison, T. F. Whale, M. A. Carpenter, M. A. Holden, L. Neve, D. O'Sullivan, J. Vergara Temprado and B. J. Murray, Not all feldspars are equal: a survey of ice nucleating properties across the feldspar group of minerals, *Atmos. Chem. Phys.*, 2016, **16**, 10927–10940.

58 T. Zolles, J. Burkart, T. Häusler, B. Pummer, R. Hitzenberger and H. Grothe, Identification of Ice Nucleation Active Sites on Feldspar Dust Particles, *J. Phys. Chem. A*, 2015, **119**, 2692–2700.

59 A. Kiselev, F. Bachmann, P. Pedevilla, S. J. Cox, A. Michaelides, D. Gerthsen and T. Leisner, Active sites in heterogeneous ice nucleation—the example of K-rich feldspars, *Science*, 2017, **355**, 367–371.

60 J. D. Atkinson, B. J. Murray, M. T. Woodhouse, T. F. Whale, K. J. Baustian, K. S. Carslaw, S. Dobbie, D. O'Sullivan and T. L. Malkin, The importance of feldspar for ice nucleation by mineral dust in mixed-phase clouds, *Nature*, 2013, **498**, 355–358.

61 J. Vergara-Temprado, B. J. Murray, T. W. Wilson, D. O'Sullivan, J. Browse, K. J. Pringle, K. Ardon-Dryer, A. K. Bertram, S. M. Burrows, D. Ceburnis, P. J. DeMott, R. H. Mason, C. D. O'Dowd, M. Rinaldi and K. S. Carslaw, Contribution of feldspar and marine organic aerosols to global ice nucleating particle concentrations, *Atmos. Chem. Phys.*, 2017, **17**, 3637–3658.

62 Y. Boose, A. Welti, J. Atkinson, F. Ramelli, A. Danielczok, H. G. Bingemer, M. Plötze, B. Sierau, Z. A. Kanji and U. Lohmann, Heterogeneous ice nucleation on dust particles sourced from nine deserts worldwide – Part 1: Immersion freezing, *Atmos. Chem. Phys.*, 2016, **16**, 15075–15095.

63 A. D. Harrison, K. Lever, A. Sanchez-Marroquin, M. A. Holden, T. F. Whale, M. D. Tarn, J. B. McQuaid and B. J. Murray, The ice-nucleating ability of quartz immersed in water and its atmospheric importance compared to K-feldspar, *Atmos. Chem. Phys.*, 2019, **19**, 11343–11361.

64 M. Niemand, O. Möhler, B. Vogel, H. Vogel, C. Hoose, P. Connolly, H. Klein, H. Bingemer, P. DeMott, J. Skrotzki and T. Leisner, A Particle-Surface-Area-Based Parameterization of Immersion Freezing on Desert Dust Particles, *J. Atmos. Sci.*, 2012, **69**, 3077–3092.

65 P. J. Connolly, O. Möhler, P. R. Field, H. Saathoff, R. Burgess, T. Choularton and M. Gallagher, Studies of heterogeneous freezing by three different desert dust samples, *Atmos. Chem. Phys.*, 2009, **9**, 2805–2824.

66 A. Hodson, A. M. Anesio, M. Tranter, A. Fountain, M. Osborn, J. Priscu, J. Laybourn-Parry and B. Sattler, GLACIAL ECOSYSTEMS, *Ecol. Monogr.*, 2008, **78**, 41–67.

67 M. Stibal, M. Šabacká and J. Žárský, Biological processes on glacier and ice sheet surfaces, *Nat. Geosci.*, 2012, **5**, 771–774.

68 E. Hood, T. J. Battin, J. Fellman, S. O'Neel and R. G. M. Spencer, Storage and release of organic carbon from glaciers and ice sheets, *Nat. Geosci.*, 2015, **8**, 91–96.

69 M. D. Petters and T. P. Wright, Revisiting ice nucleation from precipitation samples, *Geophys. Res. Lett.*, 2015, **42**, 8758–8766.

70 E. K. Bigg, Ice forming nuclei in the high Arctic, *Tellus, Ser. B Chem. Phys. Meteorol.*, 1996, **48**, 223–233.

71 R. H. Mason, M. Si, C. Chou, V. E. Irish, R. Dickie, P. Elizondo, R. Wong, M. Brintnell, M. Elsasser, W. M. Lassar, K. M. Pierce, W. R. Leaitch, A. M. MacDonald, A. Platt, D. Toom-Sauntry, R. Sarda-Estève, C. L. Schiller, K. J. Suski, T. C. J. Hill, J. P. D. Abbatt, J. A. Huffman, P. J. DeMott and A. K. Bertram, Size-resolved measurements of ice-nucleating particles at six locations in North America and one in Europe, *Atmos. Chem. Phys.*, 2016, **16**, 1637–1651.

72 L. F. Radke, P. V. Hobbs and J. E. Pinnons, Observations of Cloud Condensation Nuclei, Sodium-Containing Particles,

Ice Nuclei and the Light-Scattering Coefficient Near Barrow, Alaska, *J. Appl. Meteorol.*, 1976, **15**, 982–995.

73 E. K. Bigg and C. Leck, Cloud-active particles over the central Arctic Ocean, *J. Geophys. Res. Atmos.*, 2001, **106**, 32155–32166.

74 F. Conen, E. Stopelli and L. Zimmermann, Clues that decaying leaves enrich Arctic air with ice nucleating particles, *Atmos. Environ.*, 2016, **129**, 91–94.

75 A. G. Fountain and T. Ohtake, Concentrations and Source Areas of Ice Nuclei in the Alaskan Atmosphere, *J. Clim. Appl. Meteorol.*, 1985, **24**, 377–382.

76 T. Koop, B. Luo, U. M. Biermann, P. J. Crutzen and T. Peter, Freezing of HNO 3/H 2 SO 4/H 2 O Solutions at Stratospheric Temperatures: Nucleation Statistics and Experiments, *J. Phys. Chem. A*, 1997, **101**, 1117–1133.

77 P. J. DeMott, O. Möhler, D. J. Cziczo, N. Hiranuma, M. D. Petters, S. S. Petters, F. Belosi, H. G. Bingemer, S. D. Brooks, C. Budke, M. Burkert-Kohn, K. N. Collier, A. Danielczok, O. Eppers, L. Felgitsch, S. Garimella, H. Grothe, P. Herenz, T. C. J. Hill, K. Höhler, Z. A. Kanji, A. Kiselev, T. Koop, T. B. Kristensen, K. Krüger, G. Kulkarni, E. J. T. Levin, B. J. Murray, A. Nicosia, D. O'Sullivan, A. Peckhaus, M. J. Polen, H. C. Price, N. Reicher, D. A. Rothenberg, Y. Rudich, G. Santachiara, T. Schiebel, J. Schrod, T. M. Seifried, F. Stratmann, R. C. Sullivan, K. J. Suski, M. Szakáll, H. P. Taylor, R. Ullrich, J. Vergara-Temprado, R. Wagner, T. F. Whale, D. Weber, A. Welti, T. W. Wilson, M. J. Wolf and J. Zenker, The Fifth International Workshop on Ice Nucleation phase 2 (FIN-02): laboratory intercomparison of ice nucleation measurements, *Atmos. Meas. Tech.*, 2018, **11**, 6231–6257.